

DEGENERATION OF LUMP-TYPE LOCALIZED WAVES IN THE (2+1)-DIMENSIONAL ITO EQUATION*

Xiaoxue Zhang¹, Chuanjian Wang^{1,2,†}, Changzhao Li¹
and Lirong Wang¹

Dedicated to Professor Jibin Li on the occasion of his 80th birthday.

Abstract The degeneration of lump-type localized waves in the (2+1)-dimensional Ito equation is investigated through the parallel relationship of wave numbers. These lump-type localized waves can degenerate into three different kinds of localized wave solutions: singular lump-type localized wave, periodic variable amplitude localized wave, rogue wave. In the process of propagation, the lump-type localized waves keep the same waveform structure and amplitude. However, the periodic variable amplitude localized wave demonstrates three different kinds of waveform structures, which presents an interesting emit-absorb interaction phenomenon. By an emitting and absorbing interaction, the localized wave realizes the energy exchange from one localized wave to another, and keeps the original waveform structure. Rogue wave is a rational growing-and-decaying localized wave which is localized in both space and time.

Keywords (2+1)-dimensional Ito equation, lump-type localized wave, degeneration, rogue wave.

MSC(2010) 35Q51, 35Q53, 35C99.

1. Introduction

In the study describing the evolution of shallow gravity waves, Ito equation [1, 10, 24, 31]

$$u_{tt} + u_{xxxxt} + 3(uu_{xt} + 2u_xu_t) + 3u_{xx} \int_{-\infty}^x u_t dx' = 0, \quad (1.1)$$

plays a crucial role in different fields of nonlinear wave, which can be used to describe all kinds of nonlinear wave phenomena, for instance internal gravity waves in fluid mechanics, rogue waves in condensed matter physics, nonlinear ion acoustic waves in quantum plasmas and so on. Through the recursion operator [7], Ito model was

[†]The corresponding author. Email: wcyj20082002@aliyun.com (C. Wang)

¹Department of Mathematics, Kunming University of Science and Technology, Kunming 650500, China

²Research center for Mathematics and Interdisciplinary Sciences, Kunming University of Science and Technology, Kunming 650500, China

*The authors were supported by National Natural Science Foundation of China (11801240).

also derived by Drinfeld and Sokolov in the following form

$$\begin{cases} u_t = v_x, \\ v_t + 3(uv)_x + v_{xxx} = 0, \end{cases} \tag{1.2}$$

which is referred to as Drinfeld-Sokolov system [2, 14, 32]. In order to investigate the evolution of high-dimensional nonlinear shallow waves, Ito [10] also derived the (2+1)-dimensional Ito equation [6, 8, 15–22, 25, 26, 30, 33]

$$u_{tt} + u_{xxx} + 3(uu_{xt} + 2u_x u_t) + 3u_{xx} \int_{-\infty}^x u_t dx' + \alpha u_{yt} + \beta u_{xt} = 0, \tag{1.3}$$

where $u = u(x, y, t)$ is a real differentiable function, x and y denote the spatial variables, the variable t denotes time. α and β are two real parameters. The (2+1)-dimensional Ito equation can be used to describe nonlinear rolling of a ship, and also investigate the collision and interaction between two internal long waves. On the basis of the logarithmic transformation $u = 2(\ln F)_{xx}$, (1.3) can be converted into the Hirota differential equation

$$(D_t^2 + D_x^3 D_t + \alpha D_y D_t + \beta D_x D_t) F \cdot F = 0, \tag{1.4}$$

where the Hirota derivative D [9] is defined by

$$D_t^m D_x^n D_y^l f \cdot g = (\partial_t - \partial_{t'})^m (\partial_x - \partial_{x'})^n (\partial_y - \partial_{y'})^l [f(x, y, t)g(x', y', t')] \Big|_{(x', y', t')=(x, y, t)},$$

and m , n and l are some nonnegative integers. Through the Hirota differential equation (1.4), many authors constructed multiple solitary wave solutions, breather wave solutions, lump solution and investigated their interactions [6, 8, 15, 16, 18–20, 25, 30]. Wang shown the transition mechanism of breather wave [26]. Tan and Zha discussed mixing localized wave solutions [21, 22]. In [34], the authors investigated the high-order lump-type localized waves and their interactions. But despite all that, studying the degeneration of lump-type localized waves has not been reported in the (2+1)-dimensional Ito equation. Hence the main goal of this paper is to investigate the degeneration mechanism of lump-type localized waves.

The paper is arranged as follows. In section 2, we will present the linear representation and localized wave solutions of the (2+1)-dimensional Ito equation. Next, through analysis for the parallel relationship of wave numbers, we discuss the degeneration of lump-type localized wave chain. Three different kinds of localized wave solutions, including singular lump-type localized wave, periodic variable amplitude localized wave and rogue wave, are displayed. Finally conclusions will be given.

2. Linear representation and exponential type localized waves

In order to investigate the degeneration mechanism of lump-type localized waves for the (2+1)-dimensional Ito equation, we introduce a new dependent variable $v = v(x, y, t)$ and an auxiliary parameter γ in (1.3)

$$u_t = (v + \gamma)_x, \tag{2.1}$$

then the (2+1)-dimensional Ito equation can be translated into the system

$$\begin{cases} u_t = v_x, \\ v_t + \alpha v_y + \beta v_x + 3\gamma u_x + 3(uv)_x + v_{xxx} = 0. \end{cases} \quad (2.2)$$

Further, by using the dependent variable transformation

$$\begin{cases} u = 2(\ln F)_{xx}, \\ v = 2(\ln F)_{xt}, \end{cases} \quad (2.3)$$

one can convert the system (2.2) into the Hirota differential equation

$$P(D)F \cdot F = (D_x^3 D_t + \alpha D_y D_t + \beta D_x D_t + 3\gamma D_x^2 + D_t^2)F \cdot F = 0, \quad (2.4)$$

where $F = F(x, y, t)$ is an auxiliary function to be determined later. Obviously, when $\gamma = 0$, the Hirota differential equation (2.4) reduces to (1.4). Therefore, the system (2.2) is a generalization of the (2+1)-dimensional Ito equation. In the discussion below, one mainly investigates the degeneration mechanism of lump-type localized waves under the parameter γ control in (2.2).

In order to solve the Hirota differential equation, we expand the auxiliary function $F(x, y, t)$ as the power series

$$F = \sum_{k=0}^{\infty} \varepsilon^k f_k, \quad (2.5)$$

where $f_0 = 1$, $f_k = f_k(x, y, t)$ and ε is an arbitrary parameter. Substituting (2.5) into (2.4), and collecting terms in the resulting equation at each order of ε , one can derive the following linear equations

$$\sum_{i=0}^n P(D)f_{n-i} \cdot f_i = 0, n = 0, 1, 2, 3, \dots \quad (2.6)$$

Based on the characteristics of the linear equations (2.6), we can derive the exponential function solution

$$F_n(x, y, t) = \sum_{\mu_i=0,1} e^{i=1} \sum_{i=1}^n \mu_i \xi_i + \sum_{i<j}^n \mu_i \mu_j \delta_{ij}, \quad \xi_i = p_i x + q_i y + c_i t, \quad (2.7)$$

where the wave number (p_i, q_i) , the frequency c_i , and the phase δ_{ij} are defined as follows

$$\begin{aligned} c_i^2 + (p_i^3 + \alpha q_i + \beta p_i)c_i + 3\gamma p_i^2 &= 0, \\ \delta_{ij} &= \ln \frac{\gamma(p_i c_j - c_i p_j)^2 - c_i c_j p_i p_j (p_i - p_j)(c_i - c_j)}{\gamma(p_i c_j - c_i p_j)^2 - c_i c_j p_i p_j (p_i + p_j)(c_i + c_j)}. \end{aligned}$$

Through the dependent variable transformation (2.3), one can obtain the exponential type localized wave solutions of the system (2.2). This kind of localized wave solution has been discussed in Ref. [34]. In the section that follow, we mainly derive the lump-type localized wave chain through (2.7) and discuss their dynamic behaviors.

3. Lump-type localized wave chain and its degeneration

This section mainly derive the lump-type localized wave chain and investigate its degeneration. In order to construct the lump-type localized wave chain, choosing the following parameters in (2.7)

$$n = 2, p_1 = \bar{p}_2 = a_1 + \mathbf{i}b_1, q_1 = \bar{q}_2 = m_1 + \mathbf{i}n_1, c_1 = \bar{c}_2 = d_1 + \mathbf{i}l_1,$$

where $\mathbf{i}^2 = -1$, $a_1, b_1, m_1, n_1, d_1, l_1$ are some real parameters, the symbol “-” denotes complex conjugation, then we can derive the following solution

$$u = 2\partial_x^2 \ln(\sqrt{A_{12}} \cosh(\eta + \ln \sqrt{A_{12}}) + \cos \tau), \tag{3.1}$$

where the variable η, τ and the wave velocity (v_x, v_y) are defined by

$$\begin{aligned} \eta &= a_1(x - v_x t) + m_1(y - v_y t), \tau = b_1(x - v_x t) + n_1(y - v_y t), \\ (v_x, v_y) &= \frac{1}{b_1 m_1 - a_1 n_1} (d_1 n_1 - l_1 m_1, a_1 l_1 - b_1 d_1), \end{aligned} \tag{3.2}$$

the wave numbers $(a_1, m_1), (b_1, n_1)$, the frequency d_1, l_1 , and the phase A_{12} satisfy the following relationships

$$\begin{aligned} A_{12} &= \frac{(a_1 l_1 - b_1 d_1)^2 \gamma - b_1 l_1 (d_1^2 + l_1^2) (a_1^2 + b_1^2)}{(a_1 l_1 - b_1 d_1)^2 \gamma + a_1 d_1 (d_1^2 + l_1^2) (a_1^2 + b_1^2)}, \\ (d_1^2 + l_1^2) (a_1^3 - 3a_1 b_1^2 + \alpha m_1 + \beta a_1 + d_1) + 3((a_1^2 - b_1^2) d_1 + 2a_1 b_1 l_1) \gamma &= 0, \\ (d_1^2 + l_1^2) (3a_1 b_1^2 - b_1^3 + \alpha n_1 + \beta b_1 + l_1) - 3((a_1^2 - b_1^2) l_1 - 2a_1 b_1 d_1) \gamma &= 0. \end{aligned}$$

The solution (3.1) is made up of the cosh and cos functions, and the cosh function

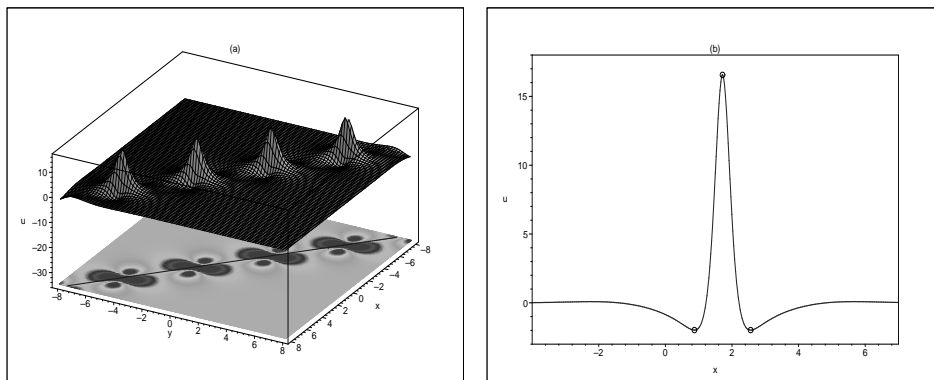


Figure 1. (a) The spatial localized structure and periodic features of the lump-type localized wave chain. (b) Sectional view in period unit showing peak and two troughs. The parameter values are $(\alpha, \beta, \gamma, a_1, b_1, d_1, l_1) = (1, 1, 1, 1, 1, 1.5, -3)$.

controls the localized structure, the periodic oscillation characteristic is governed by the cos function. Hence the solution (3.1) is a periodic oscillation localized wave

solution, which is also known as breather. If $A_{12} > 1$, that is $(a_1 d_1 + b_1 l_1)((a_1 l_1 - b_1 d_1)^2 \gamma + a_1 d_1 (d_1^2 + l_1^2)(a_1^2 + b_1^2)) < 0$, then the solution (3.1) is a nonsingular localized wave solution. For a fixed time t , the solution (3.1) is localized near the straight line $L := \eta + \ln \sqrt{A_{12}} = 0$ in the (x, y) -plane. In (3.1), when the wave numbers $(a_1, m_1), (b_1, n_1)$ satisfy the condition $\frac{a_1}{b_1} \neq \frac{m_1}{n_1}$, the solution (3.1) represents a travelling wave with the wave velocity (v_x, v_y) . This travelling wave solution is composed of a sequence of lump-type localized waves, which is called a lump-type localized wave chain. Figure 1a shows the spatial localized structure and periodic feature of the lump-type localized wave chain. As can be seen from Figure 1, this travelling wave solution is periodic along the straight line L , and made up of a series of lump-type localized waves. The period of lump-type localized wave chain along the straight line L is

$$T_l = \frac{2\pi \sqrt{a_1^2 + m_1^2}}{|a_1 n_1 - b_1 m_1|}, \quad (3.3)$$

which is the distance of two adjacent lump-type localized waves. The amplitude is $\frac{2(a_1^2 \sqrt{A_{12}} + b_1^2)}{\sqrt{A_{12}} - 1}$ and independent of the time variable t . Hence the solution (3.1) keeps the same waveform and amplitude with time evolution. The amplitude can be govern by the parameter γ . In each period unit, the singular lump-type localized wave has one peak and two troughs, see Figure 1b. When the period T_l tends to infinity, the lump-type localized wave chain degenerates into an individual lump-type localized wave which is a spatially localized travelling wave in all directions in the (x, y) -plane.

3.1. Singular lump-type localized wave

In order to derive the individual lump-type localized wave, setting the following parameters in (3.1)

$$(a_1, b_1, m_1, n_1, d_1, l_1) \rightarrow \epsilon(a_1, b_1, m_1, n_1, d_1, l_1), \eta \rightarrow \eta + i\pi,$$

where ϵ is a small parameter. Then when ϵ tends to zero, that is, the period $T_l \rightarrow \infty$, the solution (3.1) degenerates into the following rational solution

$$u = 4 \frac{(a_1^2 + b_1^2)(\eta^2 + \tau^2 + R) - 2(a_1 \eta + b_1 \tau)^2}{(\eta^2 + \tau^2 + R)^2}, \quad (3.4)$$

where the variable η, τ and the wave velocity (v_x, v_y) are given by (3.2), and the parameters $a_1, b_1, m_1, n_1, d_1, l_1, R$ satisfy the following relationships

$$\begin{aligned} R &= -\frac{(d_1^2 + l_1^2)(a_1^2 + b_1^2)(a_1 d_1 + b_1 l_1)}{\gamma(a_1 l_1 - b_1 d_1)^2}, \\ (d_1^2 + l_1^2)(\alpha m_1 + \beta a_1 + d_1) + 3(a_1^2 d_1 + 2a_1 b_1 l_1 - b_1^2 d_1)\gamma &= 0, \\ (d_1^2 + l_1^2)(\alpha n_1 + \beta b_1 + l_1) - 3(a_1^2 l_1 - 2a_1 b_1 d_1 - b_1^2 l_1)\gamma &= 0. \end{aligned}$$

The solution (3.4) is a rational polynomial function which is rationally decaying in all directions in the (x, y) -plane. When $R > 0$ and $\frac{a_1}{b_1} \neq \frac{m_1}{n_1}$, the solution (3.4) represents a nonsingular rational travelling wave with the wave velocity (v_x, v_y) , and is

called a lump-type localized wave [3, 4, 11–13, 23, 27]. This lump-type localized wave has one peak at $(v_x t, v_y t)$ and two troughs at $(v_x t \pm \frac{\sqrt{3R}}{a_1^2 + b_1^2}, v_y t)$, see Figure 2a.

The maximum is $\frac{-4\gamma(a_1 l_1 - b_1 d_1)^2}{(d_1^2 + l_1^2)(a_1 d_1 + b_1 l_1)}$, and the minimum $\frac{-\gamma(a_1 l_1 - b_1 d_1)^2}{2(d_1^2 + l_1^2)(a_1 d_1 + b_1 l_1)}$. Evidently, the amplitude of lump-type localized wave doesn't depend on the time variable t and can be govern by the parameter γ . So in the process of propagating, lump-type localized wave always keeps the same wave structure and amplitude moving forward. Besides, for a fixed moment of time t , the inclination direction of lump-type localized wave in the (x, y) -plane is determined by the line $(a_1 d_1 + b_1 l_1)t + (a_1^2 + b_1^2)x - \alpha^{-1}((a_1^2 + b_1^2)(\frac{3\gamma(a_1 d_1 + b_1 l_1)}{d_1^2 + l_1^2} + \beta) + a_1 d_1 + b_1 l_1)y = 0$. The propagation path is given by the line $xv_y - yv_x = 0$. Specifically, when $\gamma = -\frac{(\beta(a_1^2 + b_1^2) + a_1 d_1 + b_1 l_1)(d_1^2 + l_1^2)}{3(a_1^2 + b_1^2)(a_1 d_1 + b_1 l_1)}$, one can obtain the symmetric lump-type localized wave, see Figure 2b.

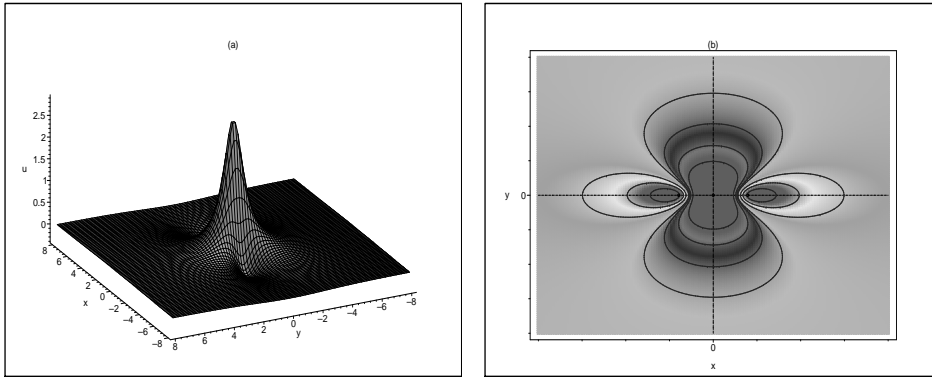


Figure 2. (a) The spatial structure structure of the singular lump-type localized wave. (b) Contour plot showing its symmetry. The parameter values are $(\alpha, \beta, \gamma, a_1, b_1, d_1, l_1) = (1, 1, \frac{5}{3}, 1, 1, 1.5, -3)$.

3.2. Periodic variable amplitude localized wave

In the discussion above, one obtained the lump-type localized wave chain and displayed its degeneration properties under the condition $\frac{a_1}{b_1} \neq \frac{m_1}{n_1}$. The results show that when the period T_l of lump-type localized wave chain tends to infinity, it will degenerate into an individual lump-type localized wave. Indeed, when $\frac{a_1}{b_1} = \frac{m_1}{n_1}$, a more interesting degeneration phenomenon will be shown.

Considering again the solution (3.1), if $\frac{a_1}{b_1} = \frac{m_1}{n_1}$, that is,

$$\gamma = \frac{(d_1^2 + l_1^2)(2a_1 b_1 (a_1^2 + b_1^2) + a_1 l_1 - b_1 d_1)}{3(a_1^2 + b_1^2)(a_1 l_1 - b_1 d_1)}, \tag{3.5}$$

then the solution (3.1) degenerates into the following form

$$u = 2\partial_x^2 \ln(\sqrt{B_{12}} \cosh(a_1 \chi + d_1 t + \ln \sqrt{B_{12}}) + \cos(b_1 \chi + l_1 t)), \tag{3.6}$$

where

$$\begin{aligned} \chi &= x - \left(\frac{\beta}{\alpha} + \frac{(a_1^2 + b_1^2)(a_1 l_1 + b_1 d_1)}{(a_1 l_1 - b_1 d_1)\alpha} + \frac{2(a_1 d_1 + b_1 l_1)}{(a_1^2 + b_1^2)\alpha} \right) y, \\ B_{12} &= \frac{(a_1 l_1 - b_1 d_1)(2a_1 b_1(a_1^2 + b_1^2) + a_1 l_1 - b_1 d_1) - 3b_1 l_1(a_1^2 + b_1^2)^2}{(a_1 l_1 - b_1 d_1)(2a_1 b_1(a_1^2 + b_1^2) + a_1 l_1 - b_1 d_1) + 3a_1 d_1(a_1^2 + b_1^2)^2}. \end{aligned} \quad (3.7)$$

The structure form of solution (3.6) is similar to that of lump-type localized wave chain (3.1), but it has completely different dynamics characteristics. When $B_{12} > 1$, it is nonsingular. The amplitude is controlled by

$$u_A(t) = \frac{2(\sqrt{B_{12}}(a_1^2 - b_1^2) \cos(\frac{(a_1 l_1 - b_1 d_1)t - b_1 \ln \sqrt{B_{12}}}{a_1}) + B_{12}a_1^2 - b_1^2)}{(\cos(\frac{(a_1 l_1 - b_1 d_1)t - b_1 \ln \sqrt{B_{12}}}{a_1}) + \sqrt{B_{12}})^2}, \quad (3.8)$$

and depends on the time variable t . Obviously, the amplitude function is a periodic oscillation function with the period

$$T_v = -\frac{2\pi a_1}{a_1 l_1 - b_1 d_1},$$

because of the \cos function. Therefore, the solution (3.6) is a periodic variable amplitude localized wave which is quite distinct from the lump-type localized wave chain (3.1). The amplitude function reaches the maximum $\frac{2(\sqrt{B_{12}}a_1^2 + b_1^2)}{\sqrt{B_{12}} - 1}$ at

$$t^* = -\frac{2(2k+1)\pi a_1 - b_1 \ln B_{12}}{2(a_1 l_1 - b_1 d_1)},$$

where $k = 0, \pm 1, \pm 2, \dots$. What is even more interesting is that the solution (3.6) will present different types of waveform structures with time evolution and different parameter conditions:

(1) When $|a_1| \geq |b_1| > 0$ and

$$\delta = ((a_1^2 + 3b_1^2)^2 - 8b_1^4)\sqrt{B_{12}} - 2(a_1^4 B_{12} + b_1^4) \leq 0,$$

the localized wave solution (3.6) will demonstrate the energy dispersal and concentration phenomena with time evolution. Figure 3 shows the evolution of wave structure in one period. When $t = -1$, the solution (3.6) represents a large amplitude W-type localized wave. Subsequently, the amplitude reduces, and the energy spreads towards two sides of the wave which causes the width of wave to increase. In particular, the amplitude achieves a minimum value at $t = -0.1$. At this point, the W-type localized wave degenerates into a small amplitude W-type localized wave. The solution (3.6) will exhibit an asymmetrical single peak localized wave between $t = -1$ and -0.1 . When $t > -0.1$, the amplitude increases, and the energy gathers toward the center of the wave. When $t = 0.8$, the amplitude reaches the maximum, and the localized wave regains the original W-type structure. In the process of propagating, through the dispersal and concentration of energy, the W-type localized wave realizes the energy exchange from one W-type localized wave to another, and keeps the original waveform structure. At the moment t^* , the amplitude of localized wave reaches the maximum value, the solution (3.6) represents a large amplitude

W-type localized wave. The amplitude of localized wave reaches the minimum value at

$$t_* = -\frac{4k\pi a_1 - b_1 \ln B_{12}}{2(a_1 l_1 - b_1 d_1)},$$

the solution (3.6) represents a small amplitude W-type localized wave. At other times the solution (3.6) will exhibit an asymmetrical single peak localized wave.

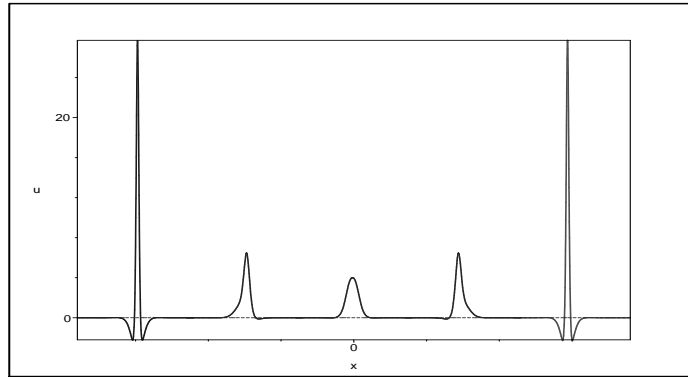


Figure 3. The waveform structures of solution (3.6) at different points of time in one period. From left to right, the point in time takes $t = -1, -0.4, -0.1, 0.3, 0.8$, respectively. The parameter values are $(\alpha, \beta, b_1, d_1, a_1, l_1) = (1, 1, 1, 1, 2, -3)$.

(2) When $|a_1| \geq |b_1| > 0$ and $\delta > 0$, the localized wave solution (3.6) will demonstrate an interesting emit-absorb interaction phenomenon with time evolution. Figure 4 shows the evolution of wave structure in one period. As can be shown from Figure 4, when $t = -0.8$, the solution (3.6) represents a large amplitude W-type localized wave. However, with the development of time, the amplitude of W-type localized wave decreases rapidly, meanwhile a small amplitude localized wave is emitted gradually from the right of W-type localized wave. Next, the amplitude of the original W-type localized wave continuously decreases, but that of new localized wave gradually increases. At this moment the solution (3.6) displays an asymmetrical double peaks localized wave structure. When $t = -0.07$, two localized waves have the same amplitude, the solution (3.6) demonstrates a M-type localized wave. Subsequently, the original W-type localized wave is absorbed gradually by new localized wave. When $t = 0.63$, the original W-type localized wave disappears, a new W-type localized wave replaces it. Indeed, throughout the whole evolutionary process, the W-type localized wave produces an interesting emit-absorb interaction phenomenon. Through an emitting and absorbing interaction, the W-type localized wave realizes the energy exchange from one W-type localized wave to another, and keeps the original waveform structure.

(3) When $0 < |a_1| < |b_1|$, the structural properties of localized wave are similar to the first two cases. However, the trigonometric function plays a crucial role in the solution (3.6) which leads to the oscillation phenomena of localized wave. When $|b_1| \gg |a_1|$, the wave oscillation strengthen evidently, the localized wave behavior weakens, see Figure 5. Conversely, it will be reduced or absent.

(4) When $a_1 \neq 0, b_1 = 0$, the structural properties of localized wave are similar to the first case. However, different from the first case, the solution (3.6) represents a small amplitude bell-type localized wave at the moment t_* because of $\delta < 0$.

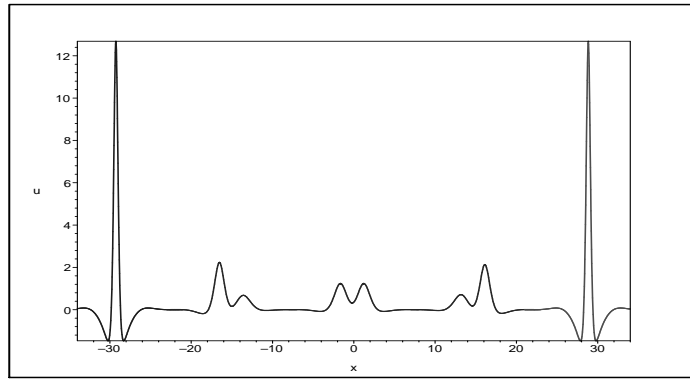


Figure 4. The waveform structures of solution (3.6) at different points of time in one period. From right to left, the point in time takes $t = -0.8, -0.2, -0.07, 0.1, 0.63$, respectively. The parameter values are $(\alpha, \beta, b_1, d_1, a_1, l_1) = (1, 1, 1, 1, 1, -3)$.

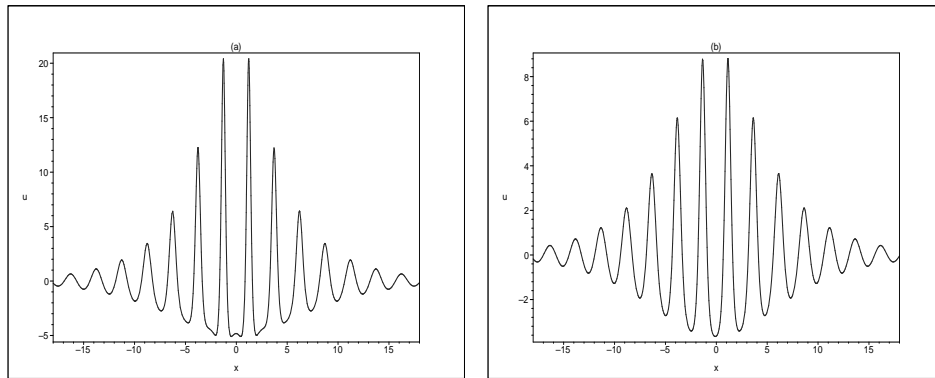


Figure 5. The oscillation phenomena of localized wave: (a) $\delta < 0$; (b) $\delta > 0$. The parameter values are $(\alpha, \beta, d_1, a_1, b_1, l_1) = (1, 1, 1, 0.2, 2.5, -0.15)$ and $(\alpha, \beta, d_1, a_1, b_1, l_1) = (1, 1, 1, 0.2, 2.5, -0.3)$, respectively.

(5) When $a_1 = 0, b_1 \neq 0$, the localized wave behavior disappears, the solution (3.6) degenerates into a growing-and-decaying periodic wave because of the function \cosh . When $|t| \rightarrow \infty$, the amplitude of periodic wave tends to zero; when $t \rightarrow \frac{-\ln B_{12} \pm 2 \operatorname{arccosh} \frac{2}{\sqrt{B_{12}}}}{2d_1}, \delta < 0$ or $t \rightarrow \frac{-\ln B_{12}}{2d_1}, \delta > 0$, the solution (3.6) represents a periodic bell-shaped wave; when $\frac{-\ln B_{12} - 2 \operatorname{arccosh} \frac{2}{\sqrt{B_{12}}}}{2d_1} < t < \frac{-\ln B_{12} + 2 \operatorname{arccosh} \frac{2}{\sqrt{B_{12}}}}{2d_1}, \delta < 0$, the solution (3.6) displays a periodic W-shaped wave. At other times, the solution (3.6) represents a small amplitude sine-like periodic wave.

(6) When $a_1 \rightarrow 0, b_1 \rightarrow 0$, the solution (3.6) degenerates into a rational growing-and-decaying localized wave, please see the below analysis.

3.3. Rogue wave

In the previous section, we have discussed the dynamical properties of lump-type localized wave chain, and obtained two kinds of degeneration solutions: lump-type localized wave and periodic variable amplitude localized wave. Now let's further consider the lump-type localized wave chain, we will derive another kind of localized wave.

Considering again the solution (3.4), if $\frac{a_1}{b_1} = \frac{m_1}{n_1}$, that is,

$$\gamma = \frac{(d_1^2 + l_1^2)}{3(a_1^2 + b_1^2)}, \tag{3.9}$$

then the solution (3.4) degenerates into the following form

$$u = \frac{4((a_1^2 + b_1^2)((a_1 z + d_1 t)^2 + (b_1 z + l_1 t)^2 + r) - 2(a_1(a_1 z + d_1 t) + b_1(b_1 z + l_1 t))^2)}{((a_1 z + d_1 t)^2 + (b_1 z + l_1 t)^2 + r)^2}, \tag{3.10}$$

where

$$z = x - \alpha^{-1}(\beta + \frac{2(a_1 d_1 + b_1 l_1)}{(a_1^2 + b_1^2)})y, r = -\frac{3(a_1^2 + b_1^2)^2(a_1 d_1 + b_1 l_1)}{(a_1 l_1 - b_1 d_1)^2}. \tag{3.11}$$

Indeed, the solution (3.10) is also derived by the solution (3.6) when the periodic

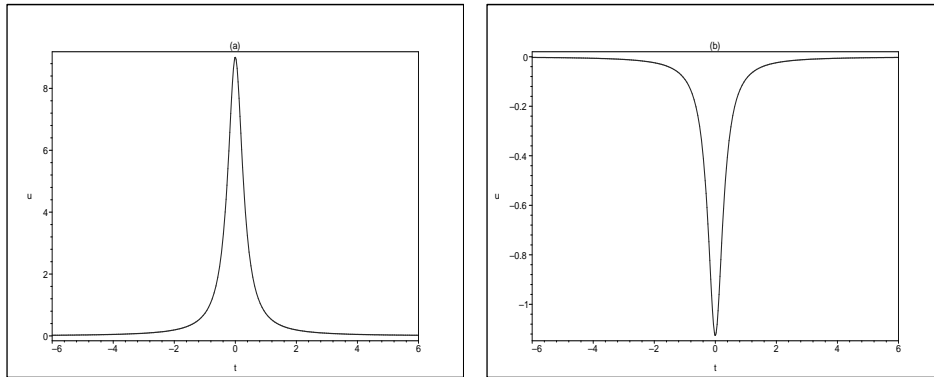


Figure 6. The time evolution plots of the maximum and minimum values: (a) $u_{max}(t)$ and (b) $u_{min}(t)$. The parameter values are $(\alpha, \beta, a_1, b_1, d_1, l_1) = (1, 1, 1, 1, 1.5, -3)$.

tends to infinity. Considering the following parameter and variable transformations in (3.6)

$$(a_1, b_1, d_1, l_1) \rightarrow \epsilon(a_1, b_1, d_1, l_1), a_1 \chi \rightarrow a_1 \chi + \mathbf{i}\pi,$$

where ϵ is a small parameter. Then when ϵ tends to zero, that is, the period $T_v \rightarrow \infty$, the solution (3.6) degenerates into the rational solution (3.10), which can be regarded as a rational polynomial function of two variables z and t and is nonsingular under the condition $r > 0$. The maximum and minimum values respectively are

$$\begin{aligned} u_{max}(t) &= \frac{4((a_1 l_1 - b_1 d_1)(a_1^2 + b_1^2))^2}{(a_1 l_1 - b_1 d_1)^4 t^2 - 3(a_1^2 + b_1^2)^3(a_1 d_1 + b_1 l_1)}, \\ u_{min}(t) &= -\frac{((a_1 l_1 - b_1 d_1)(a_1^2 + b_1^2))^2}{2((a_1 l_1 - b_1 d_1)^4 t^2 - 3(a_1^2 + b_1^2)^3(a_1 d_1 + b_1 l_1))}. \end{aligned} \tag{3.12}$$

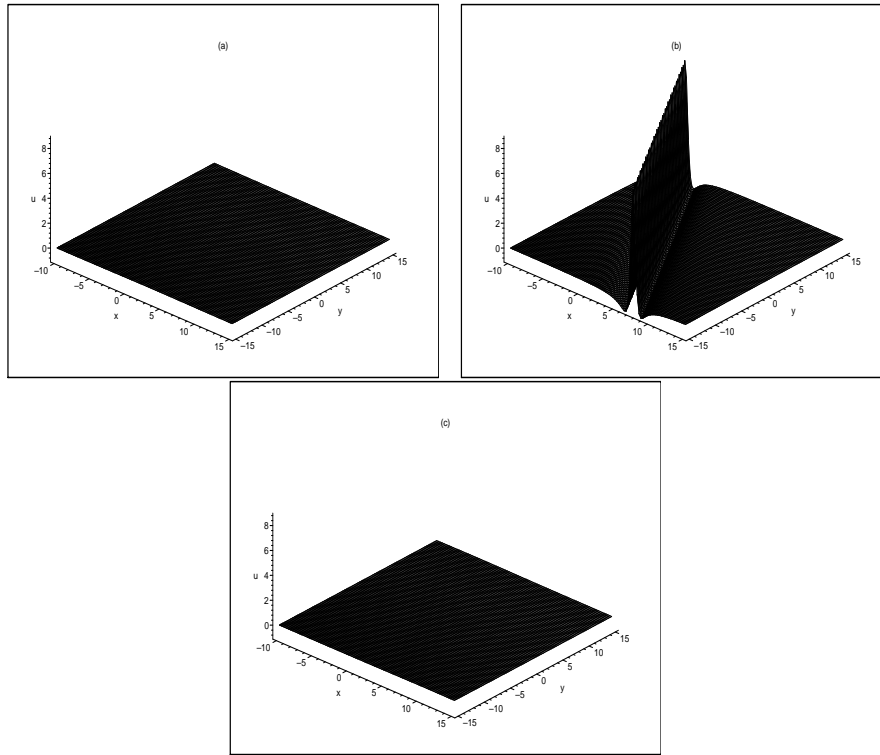


Figure 7. The spatiotemporal evolution plots of the solution (3.10): (a) $t = -5$, (b) $t = 0$ and (c) $t = 5$. The parameter values are $(\alpha, \beta, a_1, b_1, d_1, l_1) = (1, 1, 1, 1, 1.5, -3)$.

Obviously, the maximum and minimum values depend on the time variable t , and decrease quickly with time evolution, as shown in Figure 6. Hence this solution can reach the maximum amplitude $-\frac{4(a_1 l_1 - b_1 d_1)^2}{3(a_1^2 + b_1^2)(a_1 d_1 + b_1 l_1)}$ within a very short time and disappears quickly. It can not keep the same wave shape and amplitude moving forward, which is completely different from the previous lump-type localized wave. Figure 7 shows the spatiotemporal evolution of the solution (3.10). As can be seen from Figure 7, the solution (3.10) shows a W-type localized wave [28] near the line $y = -2x$ at $t = 0$ and reaches the maximum amplitude. When $|t| \rightarrow \infty$, the solution (3.10) approaches to the constant background $u = 0$ rapidly, see Figure 7a and 7c. Hence the solution (3.10) is a rational growing-and-decaying localized wave which is localized in both space and time. This property is similar to that of rogue wave [5, 29]. Hence we can call the solution (3.10) rogue wave of the (2+1)-dimensional Ito equation.

4. Conclusion

This paper investigates the degeneration of lump-type localized waves in the (2+1)-dimensional Ito equation. Firstly, we construct the lump-type localized wave chain by using the Hirota bilinear method and discuss its dynamical feature. Secondly,

through the parallel relationship of wave numbers, we demonstrate the degeneration of lump-type localized waves. The results show that the lump-type localized wave chain can degenerate into three different kinds of localized wave solutions: singular lump-type localized wave, periodic variable amplitude localized wave, rogue wave. During the process of propagating of localized waves, the lump-type localized waves keep the same waveform structure and amplitude. However, the periodic variable amplitude localized wave demonstrates three different kinds of waveform structures, which presents actually presents an interesting emit-absorb interaction phenomenon. By an emitting and absorbing interaction, the localized wave realizes the energy exchange from one localized wave to another, and keeps the original waveform structure. Rogue wave is a rational growing-and-decaying localized wave which is localized in both space and time.

Acknowledgements

The authors greatly appreciate the editors' and the anonymous referees' careful reading and helpful suggestions which have made the manuscript a real significant improvement.

References

- [1] A. R. Adem, *The generalized (1+1)-dimensional and (2+1)-dimensional Ito equations: Multiple exp-function algorithm and multiple wave solutions*, Comput. Math. Appl., 2016, 71(6), 1248–1258.
- [2] S. Bhattar, A. Mathur, D. Kumar et al., *A new analysis of fractional Drinfeld-Sokolov-Wilson model with exponential memory*, Physica A, 2020, 537, 122578.
- [3] S. Chen and X. Lü, *Lump and lump-multi-kink solutions in the (3+1)-dimensions*, Commun. Nonlinear. Sci. Numer. Simul., 2022,109, 106103.
- [4] S. Chen, X. Lü et al., *Derivation and simulation of the M-lump solutions to two (2+1)-dimensional nonlinear equations*, Phys. Scr., 2021, 96(9), 095201.
- [5] A. Chabchoub, N. P. Hoffmann and N. Akhmediev, *Rogue Wave Observation in a Water Wave Tank*, Phys. Rev. Lett., 2011, 106(20), 204502.
- [6] Y. Feng, B. Sudao and X. Wang, *Diverse exact analytical solutions and novel interaction solutions for the (2+ 1)-dimensional Ito equation*, Phys. Scr., 2020, 95(9), 095201.
- [7] M. Gürses, A. Karasu and V. V. Sokolov, *On construction of recursion operators from Lax representation*, J. Math. Phys., 1999, 40(12), 6473–6490.
- [8] C. He, Y. Tang, W. Ma and J. Ma, *Interaction phenomena between a lump and other multi-solitons for the (2+1)-dimensional BLMP and Ito equations*, Nonlinear Dyn., 2019, 95(1), 29–42.
- [9] R. Hirota, *The direct method in soliton theory*, Cambridge University Press, Cambridge, UK, 2004.
- [10] M. Ito, *An extension of nonlinear evolution equations of the KdV (mKdV) type to higher orders*, J. Phys. Soc. Jpn., 1980, 49(2), 771–778.

- [11] X. Lü and S. Chen, *New general interaction solutions to the KPI equation via an optional decoupling condition approach*, Commun. Nonlinear. Sci. Numer. Simul., 2021, 103, 105939.
- [12] X. Lü and S. Chen, *Interaction solutions to nonlinear partial differential equations via Hirota bilinear forms: one-lump-multi-stripe and one-lump-multi-soliton types*, Nonlinear Dyn., 2021, 103(1), 947–977.
- [13] X. Lü, Y. Hua et al., *Integrability characteristics of a novel (2+1)-dimensional nonlinear model: Painlevé analysis, soliton solutions, Bäcklund transformation, Lax pair and infinitely many conservation laws*, Commun. Nonlinear. Sci. Numer. Simul., 2021, 95, 105612.
- [14] Q. Liu, *Hamiltonian structures for Ito's equation*, Phys. Lett. A, 2000, 277(1), 31–34.
- [15] D. Li and J. Zhao, *New exact solutions to the (2+1)-dimensional Ito equation: Extended homoclinic test technique*, Appl. Math. Comput., 2009, 215(5), 1968–1974.
- [16] W. Ma, X. Yong and H. Zhang, *Diversity of interaction solutions to the (2+1)-dimensional Ito equation*, Comput. Math. Appl., 2018, 75(1), 289–295.
- [17] H. Ma, H. Wu, W. Ma and A. Deng, *Localized interaction solutions of the (2+1)-dimensional Ito Equation*, Opt. Quantum Electron., 2021, 53(6), 1–16.
- [18] S. Tian and H. Zhang, *Riemann theta functions periodic wave solutions and rational characteristics for the (1+1)-dimensional and (2+1)-dimensional Ito equation*, Chaos Solitons Fractals, 2013, 47, 27–41.
- [19] Y. Tian and Z. Dai, *Rogue waves and new multi-wave solutions of the (2+1)-dimensional Ito equation*, Z. Naturforsch. A, 2013, 70(6), 437–443.
- [20] W. Tan, Z. Dai and H. Dai, *Dynamical analysis of lump solution for the (2+1)-dimensional Ito equation*, Therm. Sci., 2017, 21(4), 1673–1679.
- [21] W. Tan, *Some new dynamical behaviour of double breathers and lump-N-solitons for the Ito equation*, Int. J Comput. Math., 2021, 98(5), 961–974.
- [22] X. Tan and Q. Zha, *Three wave mixing effect in the (2+1)-dimensional Ito equation*, Int. J Comput. Math., 2021, 98(10), 1921–1934.
- [23] W. Tan, W. Zhang and J. Zhang, *Evolutionary behavior of breathers and interaction solutions with M-solitons for (2+1)-dimensional KdV system*, Appl. Math. Lett., 2020, 101, 106063.
- [24] A. M. Wazwaz, *Multiple-soliton solutions for the generalized (1+1)-dimensional and the generalized (2+1)-dimensional Ito equations*, Appl. Math. Comput., 2008, 202(2), 840–849.
- [25] X. Wang, S. Tian, C. Qin and T. Zhang, *Dynamics of the breathers, rogue waves and solitary waves in the (2+1)-dimensional Ito equation*, Appl. Math. Lett., 2017, 68, 40–47.
- [26] L. Wang, C. Liu, M. Li et al., *High-dimensional nonlinear wave transitions and their mechanism*, Chaos, 2020, 30(11), 113107.
- [27] C. Wang, *Spatiotemporal deformation of lump solution to (2+1)-dimensional KdV equation*, Nonlinear Dyn., 2016, 84(2), 697–702.

-
- [28] C. Wang, H. Fang and X. Tang, *State transition of lump-type waves for the (2+1)-dimensional generalized KdV equation*, *Nonlinear Dyn.*, 2019, 95(4), 2943–2961.
- [29] C. Wang, Z. Dai and C. Liu, *Interaction Between Kink Solitary Wave and Rogue Wave for (2+1)-Dimensional Burgers Equation*, *Mediterr. J. Math.*, 2016, 13(3), 1087–1098.
- [30] J. Yang, W. Ma and Z. Qin, *Lump and lump-soliton solutions to the (2+1)-dimensional Ito equation*, *Anal. Math. Phys.*, 2018, 8(3), 427–436.
- [31] Y. Zhang and D. Chen, *N-soliton-like solution of Ito equation*, *Commun. Theor. Phys.*, 2004, 42(5), 641–644.
- [32] Z. Zhao, Y. Zhang and Z. Han, *Symmetry analysis and conservation laws of the Drinfeld-Sokolov-Wilson system*, *Eur. Phys. J. Plus*, 2014, 129(7), 143.
- [33] Y. Zhang, Y. You, W. Ma and H. Zhao, *Resonance of solitons in a coupled higher-order Ito equation*, *J. Math. Anal. Appl.*, 2012, 394(1), 121–128.
- [34] X. Zhang, C. Wang and Y. Zhou, *High-order localized waves in the (2+1)-dimensional Ito equation*, *Phys. Scr.*, 2021, 96(7), 075215.